Parameter Estimation and Control of Multirotors

Cheng-Cheng Yang and Teng-Hu Cheng

***Abstract*— A controller based on integral concurrent learning (ICL) has been developed for controlling a multirotor unmanned aerial vehicle with unknown mass and moment of inertia, and it guarantees that the tracking errors and the estimation errors of the parameters asymptotically converge to zero. The condition for convergence of the estimated parameters in the developed ICL controller can be verified online or offline by utilizing the data recorded during normal operation over a period, and satisfying the condition does not require persistence of excitation. Since the dynamics of a multirotor is globally defined, the developed ICL controller ensures almost global tracking and parameter estimation. The developed control architecture can be generalized to control any multirotor of unknown mass and moment of inertia with guaranteed system stability. A stability analysis is conducted to ensure that both the tracking errors and the estimation errors of the parameters asymptotically converge to zero. The performance and efficacy of the ICL controller have been verified in experiments.**

I. Introduction

A multirotor is a type of vertical take-off-and-landing unmanned aerial vehicle that has enormous potential due to its agility, mobility, lightness, and maneuverability. These advantages have resulted in multirotors being widely utilized in various fields, including cooperative load transportation [1], search and rescue [2], military surveillance [3], [4], and tracking [5], [6]. Since the dynamics of the multirotor is highly nonlinear, knowledge of the geometric and inertia parameters is essential to achieve good control performance. The mass of the system is an important parameter influencing the translational dynamics, whereas the moment of inertia is important for the attitude control of multirotors. Several methods have been used to estimate the mass of a multirotor, such as the linear least-squares method and an extended Kalman filter (EKF). [7] estimated the mass of the whole system including the multirotor, grasper, and payload using a linear least-squares method in a multirotor used for aerial grasping. In [8], the authors designed an estimator that estimated the mass of the multirotor using only inertia measurements and pilot commands. [9] applied an EKF for estimating system dynamics that can run either online or offline, but it was designed for underwater vehicles. [10]–[12] presented methods for the online estimation of parameters of a multirotor that included the mass and other inertial properties. In [13], a learning method based on temporal convolutional network was developed to estimate the system dynamics purely from the experiences of a robot. However, the dynamics of the estimator in the aforementioned works were not included in stability analyses, and so the system stability was not guaranteed.

[14] proposed a method for estimating the moment of inertia directly from flight data. The method modified the Newton-Euler equation of motion for the rotational dynamics to derive a linear and algebraic model. The flight data were used to solve the unknown parameters by numerically differentiating the gyroscope signal, which is vulnerable to noises. Moreover, calculating the inverse of the matrix is too complicated to be performed on the on-board computers. A robust adaptive tracking controller was developed in [15], but it only guaranteed that the estimate errors of the moment of inertia to be uniformly ultimately bounded (UUB). Moreover, the condition on persistent excitation (PE) of the reference input is restrictive for adaptive controllers and often infeasible to monitor online. Furthermore, in flight control applications, PE reference inputs may cause nuisance and waste energy.

A frequency-domain approach for estimating the moment of inertia [16] can be applied equally to full-size helicopters and small multirotors. The dynamics of the system after linearization is fully described by frequency-response approaches, but the stability of the linearized system is only guaranteed around the equilibrium point. The performance of the controller may be impaired by nonlinear dynamics of the real physical system. Moreover, the model in [16] was derived for the hovering condition and the motion of the system is restricted to one axis at a time, whereas multirotors are usually required to follow a desired trajectory. [17] proposed an approach for accurately estimating physical parameters based on the maximum-likelihood estimation. However, it is not possible to determine the variations in parameters when the structure of a multirotor changes in real time. These kinds of problems were addressed in [18] by designing a real-time, on-board estimator for estimating the geometric and inertia parameters of a multirotor. This estimator is able to re-estimate the parameters as they change during the flight time. Nevertheless, that could only estimate unbiased states and parameters when the system was locally weakly observable. [19], [20], and [21] developed adaptive controller based on Lyapunov stability theory, and they were applied to multirotors with unknown system parameters, but asymptotic convergence on the parameter estimation were not guaranteed.

This work has developed an integral concurrent learning (ICL) control method that can simultaneously stabilize the multirotor and estimate the moment of inertia. ICL is extended from concurrent learning (CL), which use

This research was supported by the Ministry of Science and Technology, Taiwan (Grant Number MOST 111-2221-E-A49 -175 -MY2).

Department of Mechanical Engineering, National Yang Ming Chiao Tung University, Hsinchu, Taiwan 30010. Email: ccyang.me08g@nctu.edu.tw, tenghu@nycu.edu.tw

recorded input and output data of the system to apply batch-like updates to the parameter estimate dynamics, and ICL reformulates the CL method in terms of an integral, which removes the need to estimate state derivatives. These updates yield a negative definite, parameter estimation error term in the stability analysis, which allows parameter convergence to be established provided a finite excitation condition is satisfied [22]. By combining the controller architecture in [23] and [22], a concurrent learning method has been developed for estimating the system parameters. Not only is the control objective of attitude tracking achieved, but also the unknown moments of inertia converge to close to their true values. The main advantages of ICL controllers and the contributions of this study is that the dynamics of the estimator were incorporated in the stability analysis of a multirotor, which ensures system stability and asymptotic convergence of the estimates of the mass and the moment of inertia, which contrasts with [15].

The work is organized as follows. Section II presents the problem formulation and the notation. The controller is designed in Section III, and the closed-loop error systems and the stability analysis of the closed-loop systems are developed in Section IV. The obtained results and future work are discussed in Section VI.

II. Problem Formulation

A. Dynamics of the Multirotors

The rigid-body model for a multirotor is described by both translational and rotational dynamics formulated as

$$\dot{x} = v, \tag{1}$$

$$m\dot{v} = mge_3 - fRe_3, \tag{2}$$

$$\dot{R} = R\hat{\Omega}, \tag{3}$$

$$J\dot{\Omega} + \Omega \times J\Omega = M, \tag{4}$$

where x, $v \in \mathbb{R}^3$ represent the position and velocity in the inertial frame, respectively, and $f \in \mathbb{R}$ and $M \in \mathbb{R}^3$ are net thrust and moment control inputs, respectively, in the body-fixed frame. $R \in \mathrm{SO}(3)$ is the rotation matrix from the body-fixed frame to the inertial frame [23]. m and $g \in \mathbb{R}$ are the unknown mass of the multirotor and gravity, respectively, e_3 is an unit vector defined as $e_3 = [0, 0, 1]^T \in \mathbb{R}^3$, $\Omega = \begin{bmatrix} \Omega_1 & \Omega_2 & \Omega_3 \end{bmatrix}^T$is defined as the angular velocity of the multirotor, $\dot{\Omega}$ is the angular acceleration of the multirotor, and $\boldsymbol{J} \in \mathbb{R}^{3\times3}$ is the unknown inertia matrix of the multirotor defined as

$$J = \begin{bmatrix} J_{xx} & 0 & 0 \\ 0 & J_{yy} & 0 \\ 0 & 0 & J_{zz} \end{bmatrix}, \tag{5}$$

which is estimated in the subsequent analysis. Note that the body frame is assumed to have origin in the center of mass.

The total moment generated by the propellers in the body-fixed frame is defined as

$$M \triangleq \begin{bmatrix} M_1 \\ M_2 \\ M_3 \end{bmatrix} = \begin{bmatrix} d\left(f_4 - f_2\right) \\ d\left(f_1 - f_3\right) \\ c_{\tau f}\left(-f_1 + f_2 - f_3 + f_4\right) \end{bmatrix},$$

where f_i is the thrust generated by the i^{th} propeller along the $-\vec{Z}_B$ axis and the relation between f and f_i can be expressed as $f = \sum_{i=1}^{4} f_i$, $d > 0$ is the distance between the center of mass and the center of a propeller, and $c_{\tau f} > 0$ is a constant parameter of the propeller.

Remark 1. The dynamics defined by (1)–(4) can be extended to multirotors with different numbers of axes by replacing the allocation matrix.

B. Tracking Errors and Estimation Errors

Given a desired trajectory $x_d \in \mathbb{R}^3$, the position and velocity tracking errors are defined as

$$e_x \triangleq x - x_d, \tag{6}$$

$$e_v \triangleq v - v_d, \tag{7}$$

where $v_d \triangleq \dot{x}_d \in \mathbb{R}^3$ is the desired velocity. To address the rotational dynamics in the subsequent analysis, the attitude error function on SO(3), the attitude tracking error, and the angular velocity tracking error are defined as [23]

$$\Psi(R, R_d) \triangleq \frac{1}{2}\mathrm{tr}\left[I - R_d^T R\right], \tag{8}$$

$$e_R \triangleq \frac{1}{2}\left(R_d^T R - R^T R_d\right)^{\vee}, \tag{9}$$

$$e_\Omega \triangleq \Omega - R^T R_d \Omega_d, \tag{10}$$

where $R_d = \left[\vec{X}_{B_d}, \vec{Y}_{B_d}, \vec{Z}_{B_d}\right] \in \mathrm{SO}(3)$ is the desired attitude for the multirotor, and $(\check{\cdot}) : \mathrm{SO}(3) \to \mathbb{R}^3$ is the vee map. Angular velocity $\Omega_d = \left(R_d^T \dot{R}_d\right)^{\vee}$ can be obtained from the rotational dynamics of the multirotor as described in (3). The estimation error of the mass is defined as

$$\tilde{\theta}_m \triangleq \theta_m - \hat{\theta}_m, \tag{11}$$

where θ_m is defined as

$$\theta_m \triangleq m \in \mathbb{R}, \tag{12}$$

and $\hat{\theta}_m$ is the estimate of θ_m and is updated by $\dot{\hat{\theta}}_m$ as described below.

The moment of inertia defined in (5) is reshaped to a constant column vector θ_J defined as

$$\theta_J = \begin{bmatrix} J_{xx}, & J_{yy}, & J_{zz} \end{bmatrix}^T, \tag{13}$$

where the elements in θ_J are unknown constants to be estimated during flight. The estimation error of the moment of inertia is defined as

$$\tilde{\theta}_J \triangleq \theta_J - \hat{\theta}_J, \tag{14}$$

where $\hat{\theta}_J$ is the estimate of θ_J and is updated by $\dot{\hat{\theta}}_J$ as defined in the subsequent analysis.

C. Control Objectives

The flight controller is designed for the multirotor to track a desired trajectory x_d and desired yaw direction $\vec{X}_{B_d}$, and also estimate the unknown mass and moment of inertia of the multirotor (θ_m and θ_J) during flight. These control objectives are described as

$$\begin{cases} e_x & \to 0 \\ e_v & \to 0 \\ e_R & \to 0 \\ e_\Omega & \to 0 \\ \tilde{\theta}_m & \to 0 \\ \tilde{\theta}_J & \to 0 \end{cases} \quad \text{as} \quad t \to \infty. \tag{15}$$

III. Controller Design

To ensure that the multirotor achieves the control objectives defined in (15) as well as estimate the unknown mass and moment of inertia, translational and rotational controllers f and M are designed using an ICL-based update law, as described below.

A. Translational Controller for the Multirotor

Let the translational controller be designed as

$$f = (k_x e_x + k_v e_v + Y_m \hat{\theta}_m) \cdot Re_3, \tag{16}$$

where k_x, k_v are positive control gains, and Y_m is a regression matrix defined as $Y_m : \mathbb{R}^n \times [0, \infty) \to \mathbb{R}^{n \times m}$

$$Y_m = \begin{bmatrix} -\ddot{x}_{d_1} \\ -\ddot{x}_{d_2} \\ g - \ddot{x}_{d_3} \end{bmatrix}, \tag{17}$$

where $\ddot{x}_{d_1}$, $\ddot{x}_{d_2}$, and $\ddot{x}_{d_3} \in \mathbb{R}$ are the elements of the acceleration of the desired trajectory of the multirotor $\ddot{x}_d$.

Assumption 1. Y_m comprising gravity and the command acceleration is bounded by a positive constant $\bar{Y}_m \in \mathbb{R}_{>0}$:

$$\|Y_m\| < \bar{Y}_m.$$

Remark 2. Note that the controller designed in (16) is the net thrust obtained by projecting the force control input $\vec{f}$ into e_3 on the body frame:

$$\vec{f} = k_x e_x + k_v e_v + Y_m \hat{\theta}_m. \tag{18}$$

The translational dynamics of the multirotors defined in (2) can be rewritten as

$$fRe_3 = mge_3 - m\dot{v}, \tag{19}$$

which can be linearly parameterized to separate the known and unknown parameters as

$$fRe_3 = Y_m^{cl} \theta_m, \tag{20}$$

where $Y_m^{cl} : \mathbb{R}^n \times [0, \infty) \to \mathbb{R}^{n \times m}$ is a regression matrix defined as

$$Y_m^{cl} = \begin{bmatrix} -\ddot{x}_1 \\ -\ddot{x}_2 \\ g - \ddot{x}_3 \end{bmatrix}, \tag{21}$$

and $\hat{\theta}_m$ estimates θ_m using the ICL-based update law

$$\begin{aligned} \dot{\hat{\theta}}_m = & \underbrace{\Gamma_m Y_m^T (e_v + C_1 e_x)}_{\text{for stability}} \\ & + \underbrace{k_m^{cl} \Gamma_m \sum_{j=1}^{N_m} \left(y_m^{cl}(t_j)\right)^T \left(F - y_m^{cl}(t_j)\, \hat{\theta}_m(t_j)\right)}_{\text{for learning}}, \end{aligned} \tag{22}$$

where Γ_m, $k_m^{cl}, C_1 \in \mathbb{R}_{>0}$ are positive control gains, $t_j \in [0, t]$ is the time between the initial time and the current time, and $N_m \in \mathbb{Z}^+$ is a positive constant that characterizes the amount of data used for the ICL controller.

In (22), F and y_m^{cl} are defined as

$$F(t) \triangleq \begin{cases} 0_{n \times 1} & t \in [0, \triangle t] \\ \int_{t-\triangle t}^{t} fRe_3(\tau)\, d\tau & t > \triangle t \end{cases}, \tag{23}$$

$$y_m^{cl}(t) \triangleq \begin{cases} 0_{n \times 1} & t \in [0, \triangle t] \\ \int_{t-\triangle t}^{t} Y_m^{cl}(\tau) d\tau & t > \triangle t \end{cases}, \tag{24}$$

where $\triangle t \in \mathbb{R}$ is the time interval of integration.

Remark 3. If there is no payload, the ICL controller can be used to monitor the health condition of the motors on the multirotor. For example, if a motor is damaged or the battery voltage drops, the thrust decreases for control command. In this case, maintaining a zero tracking error requires control input command F in (22) has to increase, which can result in a larger estimated value of $\hat{\theta}_m$ based on the ICL term in (22). Therefore, an increase in the estimated mass is increasing during the flight implies that a motor may be damaged or the battery voltage has dropped. Moreover, it is not difficult to further differentiate between these two factors since the percentage battery voltage drop follows a discharge curves, whereas the thrust can drop suddenly when a motor is damaged.

Proposition 1. *$\dot{\hat{\theta}}_m$ defined in (22) is equivalent to*

$$\dot{\hat{\theta}}_m = \Gamma_m Y_m^T (e_v + C_1 e_x) + k_m^{cl} \Gamma_m \mathcal{G}_m \tilde{\theta}_m. \tag{25}$$

Integrating both sides of (20) yields

$$\int_{t-\triangle t}^{t} fRe_3(\tau)\, d\tau = \int_{t-\triangle t}^{t} Y_m^{cl}(\tau) \theta_m d\tau, \tag{26}$$

where $\mathcal{G}_m \triangleq \sum_{j=1}^{N_m} \left(y_{m,j}^{cl}\right)^T y_{m,j}^{cl}$, $\theta_m \in \mathbb{R}$ represents the constant unknown mass, and $\forall t > \triangle t$. Using the fundamental theorem of calculus and the definitions in (23) and (24) yields

$$\int fRe_3(\tau) \mid_{\tau=t} - \int fRe_3(\tau) \mid_{\tau=t-\triangle t} = y_m^{cl}(t) \theta_m. \tag{27}$$

Substituting (27) into (22) yields (25). To ensure the richness of the recorded data, the following condition is presented.

Condition 1: The recorded data are sufficiently rich so that $\mathcal{G}_m$ is full rank, i.e., Rank($\mathcal{G}_m$)=1.

B. Rotational Controller for the Multirotor

The subsequent analysis is facilitated by making Assumption 2.

Assumption 2. Similar to [23], the following assumption is made:

$$\left\| -k_x e_x - k_v e_v - Y_m \hat{\theta}_m \right\| \neq 0.$$

Let the rotational controller be designed as

$$M = -k_R e_R - k_\Omega e_\Omega - Y_J \hat{\theta}_J, \tag{28}$$

where k_R, k_Ω are positive control gains, and $Y_J : \mathbb{R}^n \times [0, \infty) \to \mathbb{R}^{n \times m}$ is a regression matrix defined as

$$Y_J = \begin{bmatrix} \overline{\Omega}_1 & \Omega_2 \cdot \Omega_3 & -\Omega_2 \cdot \Omega_3 \\ -\Omega_1 \cdot \Omega_3 & \overline{\Omega}_2 & \Omega_1 \cdot \Omega_3 \\ \Omega_1 \cdot \Omega_2 & -\Omega_1 \cdot \Omega_2 & \overline{\Omega}_3 \end{bmatrix}, \tag{29}$$

where $\overline{\Omega}_1$, $\overline{\Omega}_2$, and $\overline{\Omega}_3 \in \mathbb{R}$ are the elements of $\overline{\Omega} \in \mathbb{R}^3$ defined as

$$\overline{\Omega} \triangleq \begin{bmatrix} \overline{\Omega}_1 \\ \overline{\Omega}_2 \\ \overline{\Omega}_3 \end{bmatrix} = \hat{\Omega} R^T R_d \Omega_d - R^T R_d \dot{\Omega}_d, \tag{30}$$

where $R_d = \left[\vec{X}_{B_d}, \vec{Y}_{B_d}, \vec{Z}_{B_d} \right] \in \mathrm{SO}(3)$ and

$$\vec{Z}_{B_d} = -\frac{-k_x e_x - k_v e_v - Y_m \hat{\theta}_m}{\left\| -k_x e_x - k_v e_v - Y_m \hat{\theta}_m \right\|} \tag{31}$$

designed using an approach similar to that adopted in [23], are the desired attitude and the z-axis of the body-fixed frame of the multirotor, respectively, and $\vec{Z}_{B_d}$ exists based on Assumption 2. Based on the definitions of Y_m and θ_m and Assumption 1, the following inequalities are satisfied:

$$\| -Y_m \theta_m \| < \| Y_m \| \| \theta_m \| < \bar{Y}_m \bar{\hat{\theta}}_m < B, \tag{32}$$

where $B \in \mathbb{R}_{>0}$ is a positive constant.

To facilitate the following analysis, the rotational dynamics of the multirotors defined in (4) can be further linearly parameterized as

$$M = Y_J^{cl} \theta_J, \tag{33}$$

where $Y_J^{cl} : \mathbb{R}^n \times [0, \infty) \to \mathbb{R}^{n \times m}$ is a regression matrix defined as

$$Y_J^{cl} = \begin{bmatrix} \dot{\Omega}_1 & -\Omega_2 \cdot \Omega_3 & \Omega_2 \cdot \Omega_3 \\ \Omega_1 \cdot \Omega_3 & \dot{\Omega}_2 & -\Omega_1 \cdot \Omega_3 \\ -\Omega_1 \cdot \Omega_2 & \Omega_1 \cdot \Omega_2 & \dot{\Omega}_3 \end{bmatrix}, \tag{34}$$

and θ_J is the unknown constants to be estimated according to (13).

The last term in (28), $\hat{\theta}_J$, is updated to estimate θ_J by applying the ICL-based update law:

$$\dot{\hat{\theta}}_J(t) \triangleq \underbrace{\Gamma_J Y_J^T (e_\Omega + C_2 e_R)}_{\text{for stability}} + \underbrace{k_J^{cl} \Gamma_J \sum_{j=1}^{N_J} \left(y_J^{cl}(t_j) \right)^T \left(\overline{M}(t_j) - y_J^{cl}(t_j) \hat{\theta}_J \right)}_{\text{for learning}}, \tag{35}$$

where $k_J^{cl} \in \mathbb{R}$ is the control gain, $C_2 \in \mathbb{R}$ is a positive constant, $N_J \in \mathbb{Z}^+$ is a positive constant that characterizes the number of data used for concurrent learning, $\Gamma_J \in \mathbb{R}^{m \times m}$ is a constant gain matrix, and y_J^{cl} and $\overline{M}$ are defined as

$$y_J^{cl}(t) \triangleq \begin{cases} 0_{n \times m} & t \in [0, \triangle t] \\ \int_{t - \triangle t}^{t} Y_J^{cl}(\Omega(\tau), \tau) d\tau & t > \triangle t \end{cases}, \tag{36}$$

$$\overline{M}(t) \triangleq \begin{cases} 0_{n \times 1} & t \in [0, \triangle t] \\ \int_{t - \triangle t}^{t} M(\tau) d\tau & t > \triangle t \end{cases}. \tag{37}$$

Proposition 2. *$\dot{\hat{\theta}}_J$ defined in (35) is equivalent to*

$$\dot{\hat{\theta}}_J = \Gamma_J Y_J^T (e_\Omega + C_2 e_R) + k_J^{cl} \Gamma_J \mathcal{G}_J \tilde{\theta}_J. \tag{38}$$

Integrating both sides of (33) yields

$$\int_{t - \triangle t}^{t} M(\tau) d\tau = \int_{t - \triangle t}^{t} Y_J^{cl}(\Omega, \tau) \theta_J d\tau.$$

Using the fundamental theorem of calculus and the definitions in (37) and (36) yields

$$\int M(\tau) \mid_{\tau = t} - \int M(\tau) \mid_{\tau = t - \triangle t} = y_J^{cl}(t) \theta_J. \tag{39}$$

Substituting (39) into (35) yields (38), where $\mathcal{G}_J \triangleq \sum_{j=1}^{N_J} \left(y_{J,j}^{cl} \right)^T y_{J,j}^{cl}$ and $\tilde{\theta}_J$ is the estimation error defined in (14).

Remark 4. Implementing the estimators designed in (22) and (35) only requires the trajectory tracking errors and input and output data, and therefore has no hardware cost, which corresponds to contribution C1 listed in the Introduction section. Furthermore, the learning terms of (22) and (35) can be used to run the estimator offline since they contain only the input and output data (i.e., not tracking error terms), and their convergence can be analyzed independently of the tracking error dynamics, which corresponds to contribution C2.

To ensure the richness of the recorded data, the following condition is presented.

Condition 2: The recorded data are sufficiently rich so that $\mathcal{G}_J$ is full rank, i.e., Rank($\mathcal{G}_J$)=3.

Remark 5. The Y_J^{cl} defined in (34) is not implementable since it includes angular acceleration terms $\dot{\Omega}_1$, $\dot{\Omega}_2$, and $\dot{\Omega}_3$, which are not measurable. However, by integrating Y_J^{cl} to be y_J^{cl} as defined in (36), y_J^{cl} becomes implementable since Ω_1, Ω_2, and Ω_3 are available, which corresponds to contribution C3.

A block diagram of the ICL controller is depicted in Fig. 1.

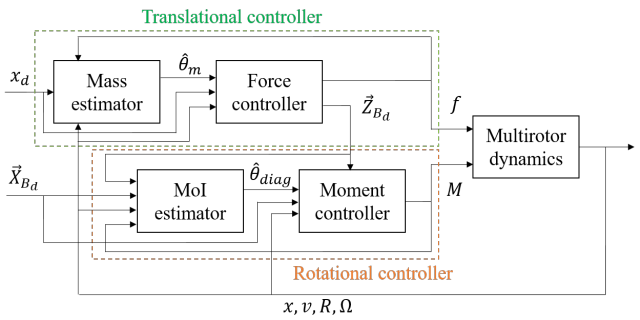

Fig. 1. Control architecture of the ICL controller. MoI, moment of inertia.

IV. Stability Analysis

To facilitate the stability analysis developed in this section, the closed-loop error systems of rotational and translational dynamics are derived first

A. Rotational Dynamics

Taking the time derivative of error dynamics e_R and e_Ω defined in (9) and (10) yields

$$\begin{aligned}\dot{e}_R &= \frac{1}{2}(R_d^T R\hat{e}_\Omega + \hat{e}_\Omega R^T R_d)^\vee \\ &= C(R_d^T R)e_\Omega, \end{aligned} \tag{40}$$

$$\begin{aligned}\dot{e}_\Omega &= \dot{\Omega} + (\hat{\Omega}R^T R_d\Omega_d - R^T R_d\dot{\Omega}_d) \\ &= \dot{\Omega} + \overline{\Omega}, \end{aligned} \tag{41}$$

where $C(R_d^T R)$ is defined as

$$C(R_d^T R) \triangleq \frac{1}{2}(\text{tr}[R^T R_d]I - R^T R_d). \tag{42}$$

Multiplying (41) by J and substituting the rotation dynamics of the multirotor (4) into (41) yields

$$J\dot{e}_\Omega = M + Y_J\theta_J,$$

where $Y_J\theta_J$ is defined as

$$Y_J\theta_J = J\overline{\Omega} - \Omega \times J\Omega, \tag{43}$$

where J, θ_J, and Y_J are defined in (5), (13), and (29), respectively.

B. Translational Dynamics

Taking the time derivative of (7) and substituting the translational dynamics of the multirotor defined in (2) yields

$$\begin{aligned}m\dot{e}_v =& mge_3 - fRe_3 - m\ddot{x}_d \\ =& Y_m\theta_m - fRe_3, \end{aligned} \tag{44}$$

where Y_m and θ_m are defined in (17) and (12). By substituting the force control (16) into (44), and adding and subtracting $\frac{f}{e_3^T R_d^T Re_3}R_d e_3$ to the right-hand side of (44) yields the closed-loop translation dynamics of the multirotor as

$$m\dot{e}_v = -k_x e_x - k_v e_v + Y_m\tilde{\theta}_m - X, \tag{45}$$

where $X \in \mathbb{R}^3$ is defined as

$$X = \frac{f}{e_3^T R_d^T Re_3}\Big(\left(e_3^T R_d^T Re_3\right)Re_3 - R_d e_3\Big).$$

The stability analysis of this control algorithm can be divided into two parts: rotational and translational. Lyapunov functions V_1 and V_2 are designed to prove the stability of the translational and rotational dynamics, respectively. The stability of the overall system is then proven by using $V = V_1 + V_2$ [24].

C. Stability Analysis of the Rotational Dynamics

Theorem 1. *The controller designed in (28) along with the update law (35) and* ***Condition 2*** *can ensure e_R and e_Ω achieve exponential stability and $\Psi\left(R\left(t\right), R_d\left(t\right)\right)$ and ψ_2 defined in (8) and (51) satisfy*

$$\Psi\left(R\left(t\right), R_d\left(t\right)\right) \leq \psi_2 < 2 \tag{46}$$

provided that the following conditions are satisfied

$$\Psi\left(R\left(0\right), R_d\left(0\right)\right) < 2 \tag{47}$$

$$\left\|e_\Omega\left(0\right)\right\|^2 < \frac{2}{\lambda_{\max}\left(J\right)}k_R\left(2 - \Psi\left(R\left(0\right), R_d\left(0\right)\right)\right). \tag{48}$$

$$\begin{aligned}C_2 < \min\Big\{&\frac{k_\Omega}{\lambda_{\max}\left(J\right)}, \frac{4k_\Omega k_R}{k_\Omega^2 + 4k_R\lambda_{\max}\left(J\right)}, \\ &\sqrt{\frac{k_R\lambda_{\min}\left(J\right)}{\lambda_{\max}\left(J\right)^2}}\Big\}, \end{aligned} \tag{49}$$

$$\begin{aligned}C_1 < \min\Big\{&\sqrt{\frac{k_x}{m}}, \frac{k_v\left(1-\alpha\right)}{m}, \\ &\frac{4k_x k_v\left(1-\alpha\right)^2}{k_v^2\left(1+\alpha\right)^2 + 4mk_x\left(1-\alpha\right)}\Big\}. \end{aligned} \tag{50}$$

where C_2 is a positive constant, and

$$\psi_2 = \frac{1}{k_R}\left[\frac{1}{2}e_\Omega\left(0\right)\cdot Je_\Omega\left(0\right) + k_R\Psi(R\left(0\right), R_d\left(0\right))\right]. \tag{51}$$

Although J in (49) is unknown, its maximal and minimal eigenvalues can be obtained from best guesses.

Let V_2 be defined as

$$\begin{aligned}V_2 =& \frac{1}{2}e_\Omega \cdot Je_\Omega + k_R\Psi(R, R_d) + JC_2e_R \cdot e_\Omega \\ &+ \frac{1}{2}\tilde{\theta}_J^T\Gamma_J^{-1}\tilde{\theta}_J, \end{aligned} \tag{52}$$

which is a positive definite function. Taking the time derivative of V_2 defined in (52) and conducting a series of algebra manipulation yields

$$\dot{V}_2 \leq -z_2^T W_2 z_2 - k_J^{cl}\tilde{\theta}_J^T\mathcal{G}_J\tilde{\theta}_J, \tag{53}$$

where W_2 is defined as

$$W_2 = \begin{bmatrix} C_2k_R & -\frac{C_2k_\Omega}{2} \\ -\frac{C_2k_\Omega}{2} & k_\Omega - C_2\lambda_{\max}(J) \end{bmatrix}, \tag{54}$$

where W_2 is positive definite by selecting C_2 to satisfy (49). Since V_2 is positive definite and $\dot{V}_2$ is negative, Theorem 1 is proven.

D. Stability Analysis of the Translational Dynamics

The proof of the stability analysis of the translational dynamics is omitted due to page limit.

E. Stability Analysis of the Overall System

Theorem 2. *The ICL controller developed in (16) and (28) along with the update laws (22) and (35) and* ***Condition 1*** *and* ***Condition 2*** *ensures that the system defined by (1)–(4) can achieve asymptotic tracking in the sense of (15) provided that C_1 and C_2 defined in (50) and (49) and the initial condition*

$$\Psi\left(R\left(0\right), R_d\left(0\right)\right) < 1 \tag{55}$$

are satisfied.

Let $V = V_1 + V_2$ be a Lyapunov function for the system containing rotational and translational dynamics:

$$\begin{aligned} V =& V_1 + V_2 \\ =& \frac{1}{2} k_x e_x^T e_x + \frac{1}{2} m e_v^T e_v + C_1 m e_x \cdot e_v \\ &+ \frac{1}{2} e_\Omega \cdot J e_\Omega + k_R \Psi\left(R, R_d\right) + J C_2 e_R \cdot e_\Omega \\ &+ \frac{1}{2} \tilde{\theta}_m^T \Gamma_m^{-1} \tilde{\theta}_m + \frac{1}{2} \tilde{\theta}_J^T \Gamma_J^{-1} \tilde{\theta}_J. \end{aligned} \tag{56}$$

Taking the time derivative of (56) yields

$$\begin{aligned} \dot{V} =& \dot{V}_1 + \dot{V}_2 \\ \leq& - z_1^T W_1 z_1 + z_1^T W_{12} z_2 - z_2^T W_2 z_2 \\ &- k_J^{cl} \tilde{\theta}_J^T \mathcal{G}_J \tilde{\theta}_J - k_m^{cl} \tilde{\theta}_m^T \mathcal{G}_m \tilde{\theta}_m, \end{aligned}$$

where matrices W_1, W_2 are positive definite and condition $\lambda_{\min}\left(W_2\right) > \frac{4\|W_{12}\|^2}{\lambda_{\min}(W_1)}$ guarantees that $\dot{V}$ is negative definite as long as the initial conditions (47) is satisfied, where W_2 is defined in (54), and therefore errors e_x, e_v, e_R, and e_Ω go to zero as time goes to infinity, as defined in (15).

Remark 6. The convergence of $\tilde{\theta}_J$ and $\tilde{\theta}_m$ is guaranteed if $\mathcal{G}_J$ and $\mathcal{G}_m$ are positive definite. Specifically, according to the definitions below (26) and (39), $\mathcal{G}_J$ and $\mathcal{G}_m$ are batch-like data and whether they are positive definite can be verified online. In contrast, in a conventional adaptive controller, the condition of convergence cannot be verified online since the regression matrix does not contain batch-like data.

V. Experiments

Experimental results obtained using the developed ICL controller on a quadcopter are presented in this section. The accuracy of the parameter estimator and the ability of the ICL controller to track a desired trajectory are demonstrated.

A. Hardware Architecture

A DJI F450 frame of multirotor is deployed as the hardware architecture to implement the ICL controller in the experiments[1]. XBee modules are equipped to the multirotor for communication between the multirotor and the ground station. Angular velocity and acceleration for obtaining the attitude of the multirotor are measured from inertial measurement unit (IMU), and the position of the multirotor is measured from motion capture system (Optitrack) with 12 cameras. The configuration of the multirotor is shown in Fig. 2.

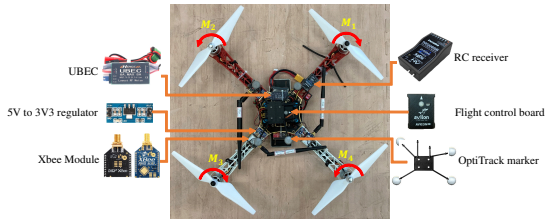

Fig. 2. Hardware architecture.

The ground truth parameters, control gains, and parameters used in ICL controller are $J = \text{diag}\left[0.013, 0.013, 0.024\right]$ kg$\cdot$m^2, $d = 0.225$ m, $m = 1.16$ kg, $k_x = 4$, $k_v = 2$, $k_R = 2.95$, $k_\Omega = 0.36$, $k_m^{cl} = 2.5$, $k_J^{cl} = 5$, $C_1 = 0.1$, $C_2 = 0.1$, and $c_{\tau f} = 1.0$. Additionally, k_x, k_v, k_R, and k_Ω are selected to be positive constants, which behave like PD gains, k_m^{cl} and k_J^{cl} are used to adjust the learning rates, and C_1 and C_2 are selected based on the inequalities provided in the proofs of Theorem 1 and Theorem 2. The constants defined in (22) and (35) are $N_m = 10$ and $N_J = 10$. The ground truth of moment of inertia is obtained by establishing the mathematical model of the multirotor and the ground truth of mass is measured on the scales. The ground truth of moment of inertia $J = \text{diag}\left[0.013, 0.013, 0.024\right]$ kg$\cdot$m^2, $d = 0.225$ m, and mass $m = 1.16$ kg were unknown parameters to be estimated in the experiments, and were used for evaluating the estimation error but not for implementing the controller.

B. Estimate of the Mass

The mass estimation of the multirotor with ICL controller converged to 1.15 kg as shown in Fig. 3 with 1% error. This means the multirotor with the developed ICL controller is able to accurately estimate the mass during the flight.

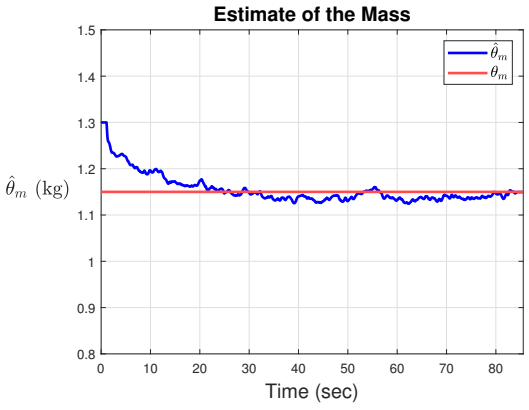

Fig. 3. Estimate of the mass of the multirotor and the ground truth.

The accurate mass estimation makes the multirotor have better tracking performance in Z direction. The comparison

[1]https://youtu.be/9IKb4pAUX2c

of the tracking errors in Z direction with geometric controller (with constant mass from best guess) and ICL controller is presented in Fig. 4. It shows that there exists steady-state error in Z direction while using geometric controller, which is caused by the voltage drop in the battery; however, the steady-state error can be eliminated by using the developed ICL controller since the $\ddot{z}$ term inside $\mathcal{G}_m$ in (22) is used for updating $\hat{\theta}_m$. In other words, the voltage drop is considered as the increase in mass in the ICL controller case, which corresponds to contribution C5.

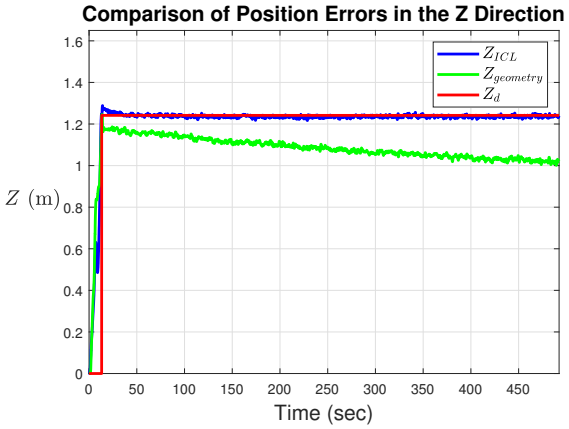

Fig. 4. Comparison of position errors in the Z direction.

C. Estimate of the Moment of Inertia

To verify the efficacy of the developed ICL controller, multiple flights with different initial estimation values of the moment of inertia were conducted. The estimation errors of the moment of inertia are presented in Fig. 5. The error can be attributed to measurement noise since this can lead to inaccurate regression matrices through integration based on (34) and (36).

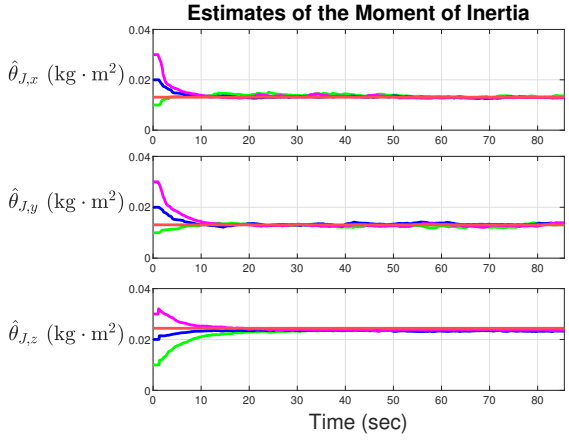

Fig. 5. Estimates of the moment of inertia. The red line indicates the ground truth, and the other lines of different colors indicate the estimates for different initial estimation values.

Moreover, the comparison between geometric controller [23], adaptive controller, and the ICL controller is presented, where the adaptive controller is similar to the ICL controller defined in (22) and (35), where only the first terms are included.

Fig. 6 compares the estimates of the moment of inertia when using an adaptive controller and the developed ICL controller. The estimation errors converged asymptotically when using the ICL controller, whereas they converged to the wrong values when using the adaptive controller.

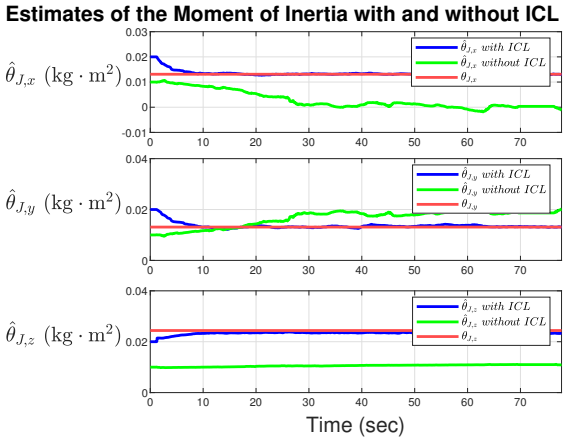

Fig. 6. Comparison of the estimation errors using the adaptive controller and the ICL controller.

D. Tracking Performance

The tracking performances of the system using the developed ICL controller and using a geometric controller are presented in Fig. 7 - 9. Compared with the geometric controllers, the multirotor with ICL controller has better tracking performance since the estimates of the mass and the moment of inertia provide system knowledge to achieve good control performance. Moreover, the mass estimate can greatly help to reduce the steady-state error in the Z direction, as shown in Fig. 9.

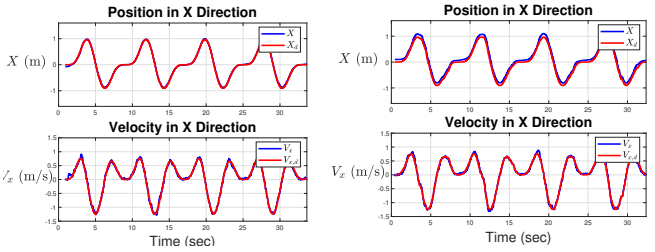

Fig. 7. Tracking errors of the position and the velocity in the X direction when (left) using the ICL controller and (right) using the geometric controller.

VI. Conclusion

An ICL controller has been developed for controlling a multirotor with unknown mass and moment of inertia. One of the main contributions of this work is that the developed ICL controller can be applied to many types of multirotors of unknown mass without the requirement of implementing extra sensors. The tracking errors and

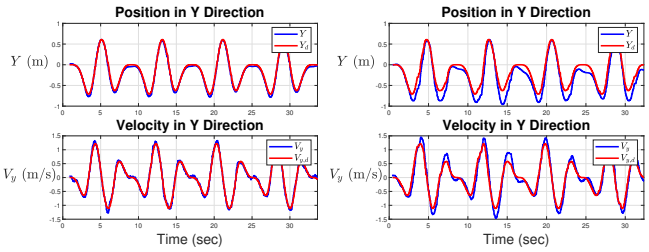

Fig. 8. Tracking errors of the position and the velocity in the Y direction when (left) using the ICL controller and (right) using the geometric controller.

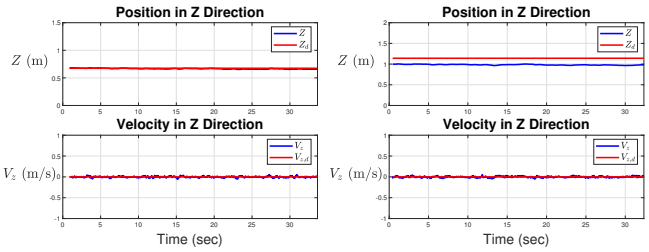

Fig. 9. Tracking errors of the position and the velocity in Z direction. Left) using the ICL controller. Right) using the geometric controller.

estimation errors of the unknown parameters have been rigorously proven to exhibit asymptotic convergence, and the stability of the ICL controller was verified in experiments. Compared with a geometric controller, the ICL controller ensures that steady-state errors in the Z direction can be greatly reduced thanks to the estimated mass. Moreover, the ICL controller can outperform an adaptive controller since the latter cannot guarantee asymptotic convergence of the system parameters in the absence of PE. Accurately estimating the system parameters using an ICL controller requires less human intervention before the flight and is thus crucial to achieving autonomous flight. The experimental results indicate that measurement noise is also an important factor when estimating the system parameters, since it can reduce the accuracy of the regression matrices.

Future work will include estimating other parameters of the multirotor, such as off-diagonal elements in the inertia matrix and the center of mass. Estimating the parameters online will avoid the need for an offline measurement procedure. Moreover, the stability of the multirotor system can still be ensured even when the geometric and inertia parameters are unknown.

REFERENCES

[1] A. S. Aghdam, M. B. Menhaj, F. Barazandeh, and F. Abdollahi, "Cooperative load transport with movable load center of mass using multiple quadrotor UAVs," in *Int. Conf. Control Instrum. Autom.*, Qazvin Islamic Azad University, Qazvin, Iran, Jan. 2016, pp. 23–27.

[2] H. A. F. Almurib, P. T. Nathan, and T. N. Kumar, "Control and path planning of quadrotor aerial vehicles for search and rescue," in *SICE Annu. Conf. 2011*, Sep. 2011, pp. 700–705.

[3] M. A. Ma'sum, M. K. Arrofi, G. Jati, F. Arifin, M. N. Kurniawan, P. Mursanto, and W. Jatmiko, "Simulation of intelligent unmanned aerial vehicle (UAV) for military surveillance," in *2013 Int. Conf. Adv. Comput. Sci. Inf. Syst.*, Sep. 2013, pp. 161–166.

[4] Z. Liu, X. Wang, L. Shen, S. Zhao, Y. Cong, J. Li, D. Yin, S. Jia, and X. Xiang, "Mission-Oriented Miniature Fixed-Wing UAV Swarms: A Multilayered and Distributed Architecture," *IEEE Trans. Syst. Man Cybern. Syst.*, pp. 1–15, 2020.

[5] Y. Liu, Q. Wang, H. Hu, and Y. He, "A novel real-time moving target tracking and path planning system for a quadrotor UAV in unknown unstructured outdoor scenes," *IEEE Trans. Syst. Man Cybern. Syst.*, vol. 49, no. 11, pp. 2362–2372, 2019.

[6] L. Zheng, F. Deng, Z. Yu, Y. Luo, and Z. Zhang, "Multilayer Neural Dynamics-Based Adaptive Control of Multirotor UAVs for Tracking Time-Varying Tasks," *IEEE Trans. Syst. Man Cybern. Syst.*, pp. 1–12, 2021.

[7] D. Mellinger, Q. Lindsey, M. Shomin, and V. Kumar, "Design, modeling, estimation and control for aerial grasping and manipulation," in *2011 IEEE/RSJ Int. Conf. Intell. Robot. Syst.*, 2011, pp. 2668–2673.

[8] D. Ho, J. Linder, G. Hendeby, and M. Enqvist, "Mass estimation of a quadcopter using IMU data," in *2017 Int. Conf. Unmanned Aircr. Syst.*, 2017, pp. 1260–1266.

[9] A. Quraishi and A. Martinoli, "Online kinematic and dynamic parameter estimation for autonomous surface and underwater vehicles," in *IEEE/RSJ Int. Conf. Intell. Robot. Syst.*, Prague, Czech Republic, Sep. 2021, pp. 4374–4381.

[10] M. A. Al-Shabi, K. S. Hatamleh, and A. A. Asad, "UAV dynamics model parameters estimation techniques: A comparison study," in *2013 IEEE Jordan Conf. Appl. Electr. Eng. Comput. Technol*, 2013, pp. 1–6.

[11] C. Böhm, C. Brommer, A. Hardt-Stremayr, and S. Weiss, "Combined System Identification and State Estimation for a Quadrotor UAV," in *IEEE Int. Conf. Robot. Autom.*, Xi'an, China, May 2021, pp. 585–591.

[12] C. Böhm, M. Scheiber, and S. Weiss, "Filter-based online system-parameter estimation for multicopter UAVs," in *Robot., Sci. Syst.*, Jul. 2021, p. 9.

[13] A. Saviolo, G. Li, and G. Loianno, "Physics-inspired temporal learning of quadrotor dynamics for accurate model predictive trajectory tracking," 2022.

[14] J. Muliadi, R. Langit, and B. Kusumoputro, "Estimating the UAV moments of inertia directly from its flight data," in *2017 15th Int. Conf. Qual. Res. (QiR) : Int. Symp. Electr. Comput. Eng.*, Jul. 2017, pp. 190–196.

[15] T. Lee, "Robust adaptive attitude tracking on SO(3) with an application to a quadrotor UAV," *IEEE Trans. Control Syst. Technol.*, vol. 21, no. 5, pp. 1924–1930, 2013.

[16] B. Mettler, M. B. Tischler, and T. Kanade, "System Identification of Small-Size Unmanned Helicopter Dynamics," in *Annu. Forum Proc. Am. Helicopter Soc.*, vol. 2, May 1999, pp. 1706 – 1717.

[17] M. Burri, M. Bloesch, Z. Taylor, R. Siegwart, and J. Nieto, "A framework for maximum likelihood parameter identification applied on MAVs," *J. Field Robot.*, vol. 35, no. 1, pp. 5–22, 2018.

[18] V. Wüest, V. Kumar, and G. Loianno, "Online estimation of geometric and inertia parameters for multirotor aerial vehicles," in *2019 Int. Conf. Robot. Autom.*, 2019, pp. 1884–1890.

[19] M. Imran Rashid and S. Akhtar, "Adaptive control of a quadrotor with unknown model parameters," in *Proc. Int. Bhurban Conf. Appl. Sci. Technol*, 2012, pp. 8–14.

[20] C. Diao, B. Xian, Q. Yin, W. Zeng, H. Li, and Y. Yang, "A nonlinear adaptive control approach for quadrotor UAVs," in *2011 8th Asian Control Conf. (ASCC)*, 2011, pp. 223–228.

[21] N. A. Chaturvedi, D. S. Bernstein, J. Ahmed, F. Bacconi, and N. H. McClamroch, "Globally convergent adaptive tracking of angular velocity and inertia identification for a 3-dof rigid body," *IEEE Trans. Control Syst. Technol.*, vol. 14, no. 5, pp. 841–853, 2006.

[22] A. Parikh, R. Kamalapurkar, and W. E. Dixon. (2015) Integral concurrent learning: Adaptive control with parameter convergence without PE or state derivatives. arXiv:1512.03464.

[23] T. Lee, M. Leok, and N. H. McClamroch, "Geometric tracking control of a quadrotor UAV on SE(3)," in *IEEE Conf. Decis. Control*, 2010, pp. 5420–5425.

[24] D. Shevitz and B. Paden, "Lyapunov stability theory of nonsmooth systems," *IEEE Trans. Autom. Control*, vol. 39 no. 9, pp. 1910–1914, 1994.